

Synthetic and structural studies of NHC–Pt(dvtms) complexes and their application as alkene hydrosilylation catalysts (NHC = N-heterocyclic carbene, dvtms = divinyltetramethylsiloxane)

Guillaume Berthon-Gelloz ^a, Olivier Buisine ^b, Jean-François Brière ^c, Guillaume Michaud ^d, Sébastien Stérin ^b, Gérard Mignani ^b, Bernard Tinant ^a, Jean-Paul Declercq ^a, David Chapon ^a, István E. Markó ^{a,*}

^a Université catholique de Louvain, Département de chimie, Bâtiment Lavoisier, Place Louis Pasteur 1, 1348 Louvain-la-Neuve, Belgium

^b Rhodia Centre de Recherche de Lyon, Av. des Frères Perret 85, F-69192 Saint-Fons Cedex, France

^c Laboratoire de Chimie Moléculaire et Thio-organique UMR CNRS 6507, ENSICAEN 6, Boulevard du Maréchal Juin, 14 050 Caen, France

^d Certech asbl, Rue Jules Bordet, Zone industrielle C, 7180 Senefte, Belgium

Received 22 June 2005; accepted 12 August 2005

Available online 23 September 2005

Abstract

The synthesis and structural characterization of a series of platinum complexes, bearing *N*-heterocyclic carbenes (NHC) and divinyltetramethylsiloxane (dvtms) as supporting ligands, are described. The reaction of commercially available Karstedt's catalyst ($\text{Pt}_2\{(\eta^2\text{-ViSiMe}_2)_2\text{O}\}_3$) with in situ generated NHC leads to monomeric platinum(0) complexes in which one NHC is bound to the metal center, as indicated by spectroscopic analysis and single-crystal X-ray diffraction studies. The relative reactivity trend for these complexes as catalysts for the hydrosilylation of alkenes is discussed in terms of NHC ligand steric properties.

© 2005 Elsevier B.V. All rights reserved.

Keywords: Platinum(0); N-Heterocyclic carbene; X-ray; Alkene; Silane; Hydrosilylation

1. Introduction

Metal NHC complexes were first described more than 40 years ago in the pioneering work of Wanzlick [1–4] and Ölefe [5]. These type of complexes were later on studied extensively by Lappert et al. [6], who reported their utility in homogeneous catalysis (e.g., ketone hydrosilylation) [7]. However, it was only during the last decade that a regain of interest in these complexes occurred with the isolation by Bertrand [8] of stable phosphinocarbenes and by Arduengo of *N*-heterocyclic carbenes [9]. Since then, there has been a steadily growing number of applications of *N*-heterocyclic carbenes as supporting ligands in homogeneous catalysis [10,11].

These substituents proved not only to be good substitutes to phosphines ligands, but in many cases have displayed superior properties to various metal templates in terms of stability and activity [12]. This is especially true for reaction carried out in the presence of oxygen, such as in aerobic oxidations, where phosphines can readily be oxidized [13].

The hydrosilylation of alkenes is one of the most atom-economical and efficient processes for the formation of alkylsilane derivatives [14–16]. Industrially, this reaction is performed under aerobic conditions and some reports even claim an accelerating effect of oxygen [17]. Therefore, in view of their stability towards air, NHCs appear to be the ideal ligands for the formation of well-defined molecular catalysts for this reaction. In previous communications, we have reported on the first synthesis of NHC–Pt(0)–divinyltetramethylsiloxane (dvtms) complexes, on their exquisite

* Corresponding author. Tel.: +32 10478773; fax: +32 1047 2788.

E-mail address: marko@chim.ucl.ac.be (I.E. Markó).

selectivity in the hydrosilylation of alkenes and on their increased functional-group tolerance, as compared to Karstedt's catalyst ($\text{Pt}_2\{(\eta^2\text{-ViSiMe}_2\text{O})_3\}$), the most efficient industrial catalyst employed today [18,19]. We now wish to present a detailed study of the structural features of an extended family of complexes of the general formula $(\text{NHC})\text{Pt}(\text{dvtms})$ ($\text{NHC} = \text{IMe}$ [N,N' -dimethylimidazol-2-ylidene] (**1**), ICy [N,N' -dicyclohexylimidazol-2-ylidene] (**2**), I^tBu [N,N' -bis(*tert*-butyl)imidazol-2-ylidene] (**3**), IAd [N,N' -bis(1-adamantyl)imidazol-2-ylidene] (**4**), IMes [N,N' -bis(2,4,6-trimethylphenyl)imidazol-2-ylidene] (**5**), IPr [N,N' -bis(2,6-diisopropylphenyl)imidazol-2-ylidene] (**6**), SIMes [N,N' -bis(2,4,6-trimethylphenyl)4,5-dihydroimidazol-2-ylidene] (**7**), SIPr [N,N' -bis(2,6-diisopropylphenyl)4,5-dihydroimidazol-2-ylidene] (**8**), BIMe [N,N' -dimethylbenzimidazol-2-ylidene] (**9**), $\text{BI}n\text{Pr}$ [N,N' -dipropylbenzimidazol-2-ylidene] (**10**), $\text{BI}m\text{Allyl}$ [N,N' -bis(methallyl)benzimidazol-2-ylidene] (**11**), $\text{BI}neo\text{Pent}$ [N,N' -bis(neopentyl)benzimidazol-2-ylidene] (**12**)). The organometallic species described are analyzed as a function of the structural features of the NHC moiety. These parameters influence the catalytic reactivity profile of this family of complexes.

2. Results and discussion

2.1. Synthesis of $(\text{NHC})\text{Pt}(\text{dvtms})$ complexes

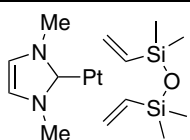
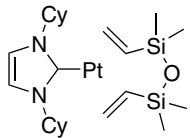
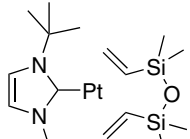
At the onset of our work, our research efforts concentrated on the synthesis of the free NHC by a methodology developed by Herrmann et al. and based upon the deprotonation of the imidazolium salt by NaH (cat. $^t\text{BuOK}$) in a NH_3/THF mixture. The NHC thus generated was then reacted with Karstedt's catalyst ($\text{Pt}_2\{(\eta^2\text{-ViSiMe}_2\text{O})_3\}$) [20,21]. This tedious protocol allowed us to isolate the first $\text{NHC-Pt}(\text{dvtms})$ complexes in reasonable yields after evaporation of the ammonia and washing the residual solid with water. Since then, a greatly simplified rendition of this protocol has been devised, which consists in suspending the imidazolium salt (1.1 eq.) with a commercially available solution of Karstedt's catalyst (1 eq. in Pt) in dry toluene, and adding $^t\text{BuOK}$ (1.1 eq.) in several portion, while stirring the light yellow mixture at room temperature for 2 h. The mixture is filtered through a pad of silica which is rinsed with P.E./ Et_2O (80/20). Evaporation of the filtrate in vacuo affords the desired complexes as white crystalline solids. This protocol has been applied to a large scale synthesis of **2** (60 g). Single crystals, suitable for X-ray diffrac-

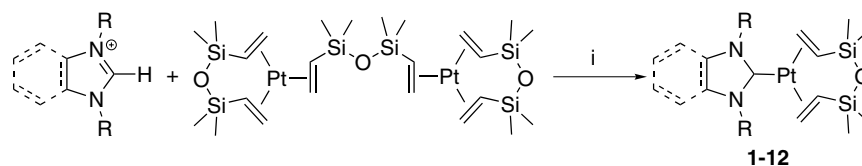
tion (XRD) studies, were obtained by slow evaporation of saturated $^t\text{PrOH}$ solutions of the metal carbenes. It is worth noting that, although the reaction is performed under an inert atmosphere, all subsequent manipulations were realized in the presence of air. These platinum(0) complexes are indefinitely stable, both as solids and in solution, when maintained under an atmosphere of air. This stability stands in stark contrast to that of other platinum(0) complexes which are relatively sensitive to air. Most of them decompose readily in solution to Pt black and must be kept in the presence of a large excess of the *dvtms* ligand to avoid their decomposition (see Scheme 1 and Tables 1–3).

2.2. Structural study of $(\text{NHC})\text{Pt}(\text{dvtms})$ complexes

Complexes **1–12** were analyzed by NMR spectroscopy and single crystals XRD. The ^1H NMR region of the vinyl silane is a very sensitive indicator of the coordination of the

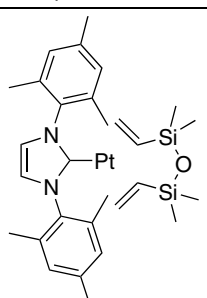
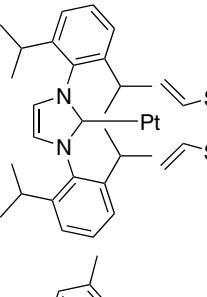
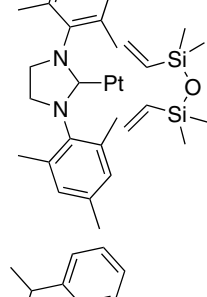
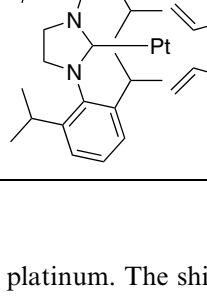
Table 1
Synthesis of alkyl substituted $(\text{NHC})\text{Pt}(\text{dvtms})$ complexes

Entry	Complex	Yield (%)
1		77
2		90
3		65
4		66



Scheme 1. Synthesis of complexes **1–12**. (i) $^t\text{BuOK}$ (1 eq.), toluene, r.t., 1–4 h.

Table 2
Synthesis of aryl substituted (NHC)Pt(dvtms) complexes

Entry	Complex	Yield (%)
1		85
2		70
3		50
4		50

dvtms ligand to platinum. The shift of the vinylsilane protons, from the 5–6 ppm region to the 1–2.5 ppm is indicative of the binding of the alkenes to the metal center. Another salient feature of the ^1H NMR is the splitting of the SiMe_2 singlet into two distinct signals for the pseudo-equatorial and pseudo-axial positions at 0.3 and –0.5 ppm, respectively. This behavior, which points towards the formation of a chelate, has been reported for complexes bearing phosphine ligands and is coherent with the XRD results as will be discussed [22]. Another important indication of the coordination of the alkene residues to platinum is the coupling of the ^{195}Pt nuclei with several protons. Thus, a $^4J_{\text{Pt-H}}$ coupling of ca. 10 Hz is observed with the imidazol-2-ylidene backbone protons and an average $^2J_{\text{Pt-H}}$ coupling of 54 Hz for the $=\text{CH}_2_{\text{eq}}$ protons. At room temperature, all the complexes, apart from **1**, **9** and

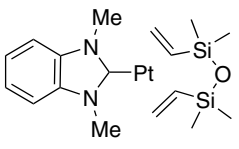
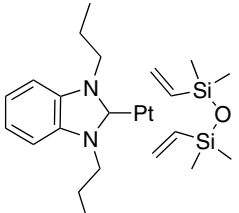
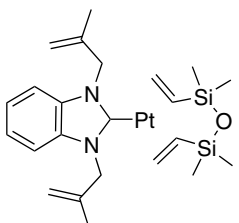
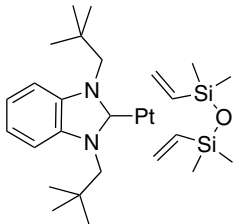
10, display diastereotopic N– CH_2 protons in their ^1H NMR spectrum, revealing the absence of rotation around the carbene–metal bond on the NMR time scale [23].

The ^{13}C NMR is also indicative of the coordination of the NHC and dvtms fragments to Pt, as evidenced through the $^{13}\text{C}/^{195}\text{Pt}$ couplings (Table 4). The ^{13}C NMR signal of the carbenic carbon appears on average at 182 ppm for the unsaturated imidazol-2-ylidene, at ca. 200 ppm for the benzimidazo-2-ylidene and at ca. 212 ppm for the saturated imidazol-2-ylidene complexes, respectively. It is interesting to note that the ^{13}C NMR shift of the benzimidazo-2-ylidene carbon is intermediate between that of the saturated imidazol-2-ylidene and unsaturated imidazol-2-ylidene derivatives. This reveals the ambivalent nature of these carbenes which bear the topology of unsaturated imidazol-2-ylidene and have the electronic factor resembling that of 4,5-dihydroimidazol-2-ylidene [24]. The carbene carbons are strongly coupled with ^{195}Pt with a $^1J_{\text{Pt-C}} = 1365$ Hz. The coupling constant between the ^{195}Pt and the carbons of the vinylic fragment of the dvtms ligand possesses a value of $^1J_{\text{Pt-C}} = 166$ Hz for the internal carbon and of 116 Hz for the terminal carbon.

The ^{195}Pt NMR spectra of these complexes provide a valuable and sensitive probe of the electronic environment of the Pt. We observed an average chemical shift of –5350 ppm for platinum (Table 5). This chemical shift is indicative of a Pt(0) complex (for reference, the chemical shift of Karstedt's catalyst is –6156 ppm) [25,26]. The literature values of ^{195}Pt of related $\text{R}_3\text{P-Pt(dvtms)}$ for $\text{R} = \text{Ph}$, Cy and $t\text{Bu}$ are –5598, –5633 and –5735 ppm, respectively [22,27]. The ^{195}Pt shifts of these complexes and the (NHC)Pt(dvtms) complexes result from the combination of two factors. The first one is the σ -donating ability of the ancillary ligand: the more electron-rich the ligand, the more downfield the ^{195}Pt shift. The second factor is back-donation of the platinum(0) center to the π^* orbital of the ancillary ligand and the alkenes. With extended back donation, the electron density on the platinum decreases and results in an upfield shift. In line with the observations reported by Nolan et al., the nature of the substituents on the NHC ligand does not alter significantly the electronic nature of the metal center. The saturated imidazo-2-ylidene complex SiPr-Pt(dvtms) (**8**) is only marginally more electron-donating (ca. 18 ppm) than the unsaturated imidazo-2-ylidene. Remarkably the most downfield shift (–5383 ppm) is observed in the case of the BnPr-Pt(dvtms) derivative (**9**). This is seemingly due to a dual effect of the low steric hindrance of the propyl substituent, which allows a closer interaction between the Pt center and the more electron-donating benzimidazo-2-ylidene framework.

In the case of (NHC)Pt(dvtms) complexes, the NHC ligand is almost solely σ -donating resulting in high electron density on the platinum center which redistributes this density onto the alkene ligand. The net result is a higher ^{195}Pt shift than the phosphine analogues and an increased stability. Hence, the ^{195}Pt shift reflects the overall reactivity of such platinum(0) complexes.

Table 3
Synthesis of alkyl substituted (BNHC)Pt(dvtms) complexes

Entry	Complex	Yield (%)
1		80
2		83
3		78
4		50

The structures of most of these complexes were unambiguously elucidated by single crystal XRD analysis (Table 6). The structures of complexes **1**, **2**, **3** and **12** have been reported in previous communications [18,19,28]. In all these organometallic derivatives, the platinum occupies the center of a trigonal planar arrangement, a coordination mode characteristic of Pt(0)(alkene)₂ complexes. Indeed, this trigonal planar conformation around platinum provides a

Table 5
¹⁹⁵Pt shift of complexes 1–10

Entry	Complex	δ ¹⁹⁵ Pt (ppm)
1	IAd–Pt(dvtms) (4)	–5306
2	ItBu–Pt(dvtms) (3)	–5333
3	IMes–Pt(dvtms) (5)	–5339
4	IPr–Pt(dvtms) (6)	–5340
5	IMe–Pt(dvtms) (1)	–5343
6	ICy–Pt(dvtms) (2)	–5343
7	SIPr–Pt(dvtms) (8)	–5361
8	SIMes–Pt(dvtms) (7)	–5365
9	BIMe–Pt(dvtms) (9)	–5379
10	BInPr–Pt(dvtms) (10)	–5383

better overlap between the Pt d-orbitals and the olefinic π^* systems, thus improving the back-bonding [29]. The dvtms ligand wraps around the platinum in a pseudochair conformation that nicely accommodates the required trigonal planar geometry around the metal. Selected bond distances are reported in Table 7.

Examination of the Pt–C_{Carbenic} distance in various members of the NHC–Pt(dvtms) family reveals only a small variation in bond length, which remains close to the mean value of 2.05 Å. The longest distance, 2.085(5) Å, is observed for (I^tBu)Pt(dvtms) and the shortest one (2.027(5) Å) is found in the case of (ICy)Pt(dvtms). These values are in agreement with a recent report by Nolan et al. [30] on a family of (NHC)Pd(Cl)allyl complexes, for which a mean Pd–C_{carbenic} distance of 2.04 Å has been measured. Such a bond length between platinum and the carbenic center correlates best with a single-bond character, in good accordance with the almost exclusive σ -donor properties of these ligands [31,32].

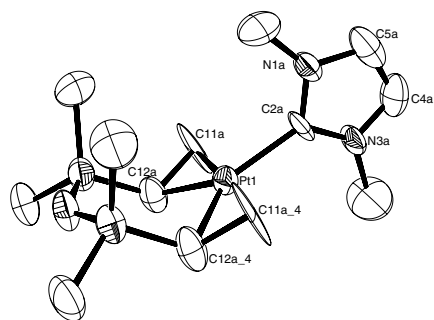
In complexes **5** and **8**, the aryl substituents adopt a “propeller” conformation around the imidazol-2-ylidene backbone. Thus, in complex **5**, the mesityl groups are tilted by 77.6(6)° and –79.2(7)°. This “fan-like” shape around the platinum center creates an unusual steric crowding which results in enhanced reactivity and selectivity [33].

The coordination features of the dvtms ligand are also excellent indicators of the strong electron-donating nature of the NHC substituents. For example, the length of the C=C bond is a good measure of the extent of back-bonding

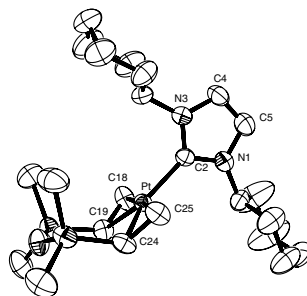
Table 4
¹³C carbene shift, J_{Pt-C} coupling and J_{Pt-H}

Entry	Complex	δ^c Pt–C _{carb}	$^1J_{Pt-C_{carb}}$	$^3J_{Pt-C_{im}}$	$^1J_{Pt-C_{vi}}$	$^1J_{Pt-C_{vi}}$	$^4J_{Pt-H_{im}}$	$^2J_{Pt-H_{vi}}$
1	IMe–Pt(dvtms) (1)	179.8					11.8	52.8
2	ICy–Pt(dvtms) (2)	180.0	1350.0	24.3	157.9	119.0	12.6	53.1
3	IAd–Pt(dvtms) (4)	180.3			185.4	123.6	12.0	53.2
4	ItBu–Pt(dvtms) (3)	181.2	1360.8	23.3	184.2	123.2	11.8	54.0
5	IMes–Pt(dvtms) (5)	184.2		41.8	165.7	117.7	9.2	55.0
6	IPr–Pt(dvtms) (6)	186.4		42.0	166.5	120.9	7.8	54.1
7	BInPr–Pt(dvtms) (10)	198.3	1373.3	41.6	158.2	113.6		54.1
8	BIMallyl–Pt(dvtms) (11)	198.3	1398.3	41.6	155.4	113.6		54.3
9	BIMe–Pt(dvtms) (9)	199.5	1377.9	39.0	155.7	113.7		54.1
10	BIneoP–Pt(dvtms) (12)	201.9	1337.0	40.7	173.3	114.0		55.0
11	SIMes–Pt(dvtms) (7)	211.0		48.0	166.3	109.7		55.5
12	SIPr–Pt(dvtms) (8)	213.3		48.4	169.2	112.8		50.6

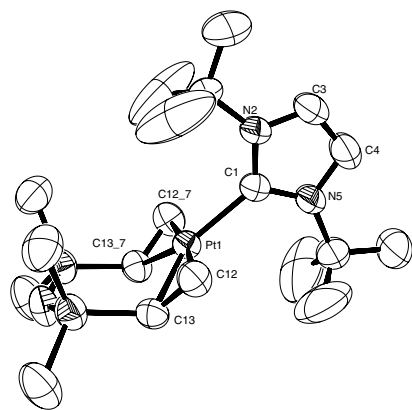
Table 6
ORTEP structure for complexes 1–3, 5, 8, 9, 11 and 12



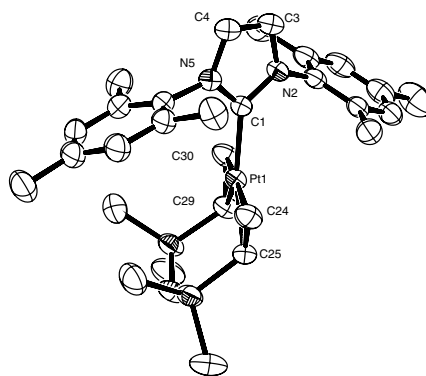
ORTEP of (Ime)Pt(dvtms) (1)



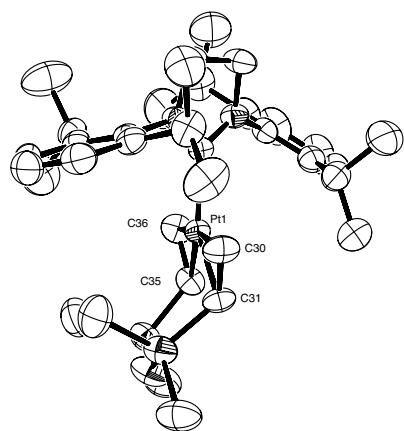
ORTEP of (ICy)Pt(dvtms) (2)



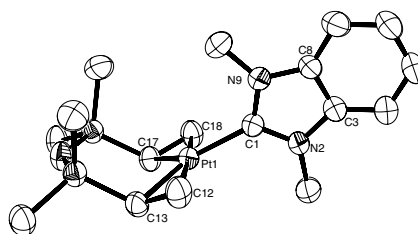
ORTEP of (*t*Bu)Pt(dvtms) (3)



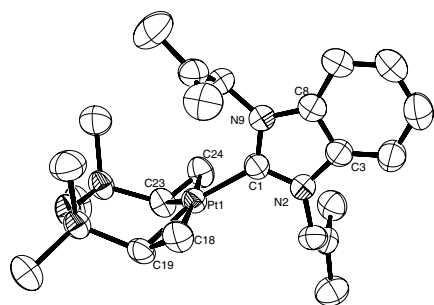
ORTEP of (IMes)Pt(dvtms) (5)



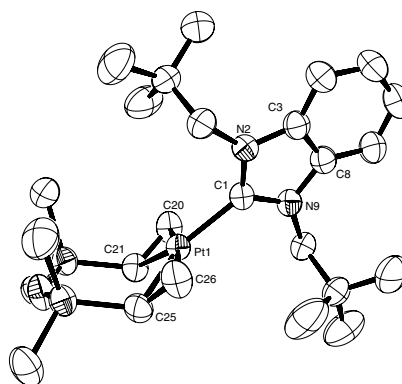
ORTEP of (SIPr)Pt(dvtms) (8)



ORTEP of (BIme)Pt(dvtms) (9)



ORTEP of (BImAllyl)Pt(dvtms) (11)



ORTEP of (BIneoPent)Pt(dvtms) (12)

Table 7
Selected structural data of all metal carbene complexes characterized by X-ray crystallography

	IMe (1)	ICy (2)	I ^t Bu (3)	IMes (5)	SIPr (8)	IBMe (9)	BImAllyl (11)	BIneoPent (12)
<i>Bond lengths (Å)</i>								
Pt–C _{carbene}	2.050(11)	2.026(5)	2.085(5)	2.046(4)	2.053(4)	2.035(4)	2.042(4)	2.058(4)
Pt–C=C ^a	2.103(15)	2.120(5)	2.130(6)	2.138(5)	2.138(6)	2.116(4)	2.127(5)	2.144(4)
Pt–C=C ^b	2.178(11)	2.136(5)	2.150(4)	2.148(5)	2.151(7)	2.143(5)	2.146(4)	2.149(4)
C _{carbene} –N ^c	1.34(2)	1.358(7)	1.361(7)	1.359(5)	1.347(6)	1.360(5)	1.351(6)	1.365(5)
C _{Im} –N ^d	1.35(2)	1.385(8)	1.371(9)	1.377(6)	1.468(6)	1.390(6)	1.398(6)	1.394(5)
C _{Im} –C _{Im} ^e	1.34(3)	1.335(10)	1.329(10)	1.332(7)	1.499(7)	1.384(6)	1.398(7)	1.387(6)
C=C–C=C ^f	1.491(13)	1.436(8)	1.433(6)	1.436(7)	1.433(7)	1.438(7)	1.421(7)	1.432(6)
C=C–C=C ^f	1.490(13)	1.420(9)	1.433(6)	1.419(7)	1.419(7)	1.428(6)	1.411(8)	1.415(7)
<i>Angles (°)</i>								
N–C _{carbene} –N	104.8(10)	103.8(5)	105.3(5)	103.1(3)	107.0(4)	105.8(3)	106.0(3)	106.0(3)
<i>Torsion (°)</i>								
N–C _{carbene} –Pt–C=C ^g	87.9(6)	82.4(9)	88.9(14)	63.8(6)	52.1(6)	88.2(4)	83.8(4)	70.3(5)
N–C _{Im} –C _{Im} –N ^h	0.0(7)	1.9(6)	0.9(12)	0.49(6)	18.2(5)	0.49(5)	0.9(4)	3.0(6)
C=C–C=C–C=C–C=C ⁱ	0.0(6)	2.4(5)	0.0(13)	4.3(6)	5.9(6)	1.1(4)	3.1(3)	1.5(5)

^a Refers to the distance of platinum to the terminal carbon.

^b Refers to the distance of platinum to the internal carbon.

^c Refers to the distance between the carbenic carbon and nitrogen.

^d Refers to the distance between the carbon of the imidazol-2-ylidene backbone and nitrogen.

^e Refers to the distance between the carbons of the imidazol-2-ylidene backbone

^f Refers to the distance between the two olefinic carbons.

^g Refers to the dihedral angle between the plane of the imidazol-2-ylidene backbone and the trigonal plane formed the dtvms ligand around the platinum center.

^h Refers to the distortion of the imidazol-2-ylidene backbone.

ⁱ Refers to the distortion from planarity of the trigonal planar arrangement of the dtvms ligand.

interactions [34]. Indeed, the mean C=C bond distance for dtvms ligand in (NHC)Pt(dtvms) complexes possesses an average value of 1.43 Å. This value, which is halfway between a double and a single bond, indicates that the olefinic linkage is particularly elongated as a result of intensive back-bonding. The longest bond length (1.491(13) Å) occurs in the case of (IMe)Pt(dtvms) (**1**), the least sterically hindered complex. This correlation between the extent of back-bonding and the average bond length of the alkene ligand is further substantiated by some of the literature data obtained for related L–Pt(0)(dtvms) complexes. Thus, the average C=C bond length for the dtvms ligand in (η^2 -1-methylnaphtoquinone)Pt(dtvms), (Pt₂{(η^2 -ViSiMe₂)₂O₃})₃, (tBu₃P)Pt(dtvms) and (Ph₃P)Pt(dtvms) are 1.37, 1.39, 1.40 and 1.40 Å, respectively [22,26,35,36].

In unhindered complexes such as **1** (87.9(6)°) and **9** (88.2(4)°), the NHC ligand is tilted by almost 90° from the plane formed by the platinum center and the SiVi substituent. This value changes dramatically when sterically encumbered ligands are employed. Hence, the NHC substituent is tilted by 82.4(9)° in **2**, 63.8(6)° in complex **5** and by 52.1(6)° in **8**. The complex (I^tBu)Pt(dtvms) (**3**) is a marked exception to this trend, with a tilt angle of the NHC of 88.9(4)°. Classified as one of the most hindered NHC ligands, this carbene should have displayed the largest tilt angle [37]. However, the spherical symmetry of the ^tBu substituents on the NHC moiety prevents the ligand from adopting a less hindered conformation by tilting the imidazol-2-ylidene backbone out of the plane perpendicular

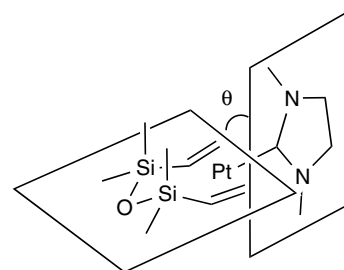


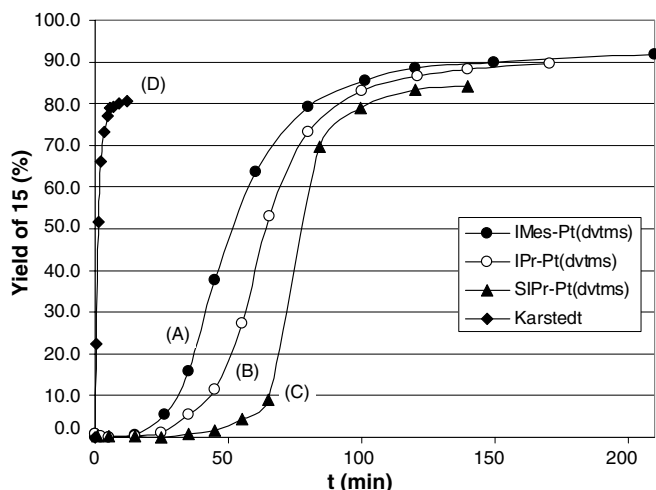
Fig. 1. View of the “tilt” θ angle of the NHC relative Pt–alkene plane.

to the Pt–SiVi plane. Instead, the release of steric strain is achieved by elongating the Pt–I^tBu bond. As a consequence, both **3** and **4** possess a weaker Pt–C linkage and are much more prone to decomposition than all the other NHC–Pt(dtvms) complexes (see Fig. 1).

We have also examined the distortion of the plane defined by the two olefinic residues of the vinylsilane ligand. This distortion appears to be linked with the tilt of the NHC substituent with respect to this plane. The more tilted the NHC, the more important is this distortion. This distortion is only significant in complexes **5** (4.6(6)°) and **8** (5.9(6)°). The distortion of the imidazol-2-ylidene backbone is particularly significant in the case of the complex SIPr–Pt(dtvms) complex (**8**) with an angle of 18.2(5)° [30].

2.3. Structure/reactivity relationship

All complexes described above were initially designed as catalysts for the hydrosilylation of alkenes. These complexes



Graph 3. Hydroosilylation of **14** by **13** catalyzed by (IMes)Pt(dvtms) curve (A), (IPr)Pt(dvtms) curve (B), (SIPr)Pt(dvtms) curve (C) and Karstedt's catalyst curve (D).

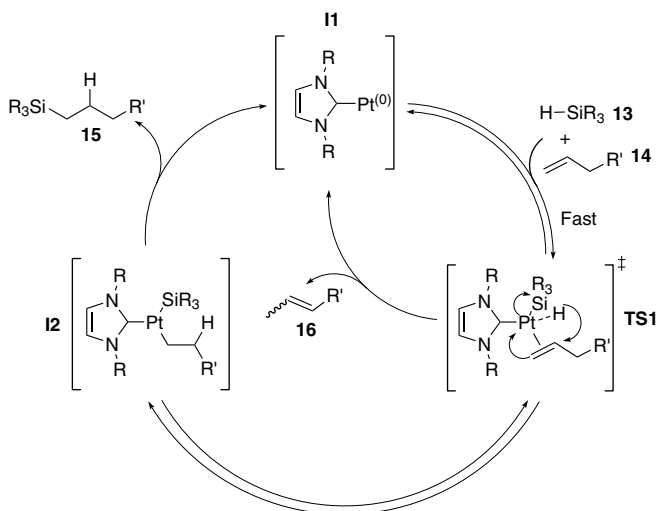
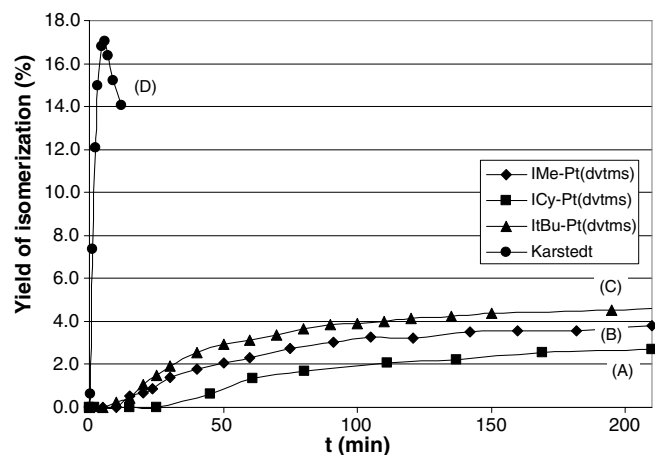


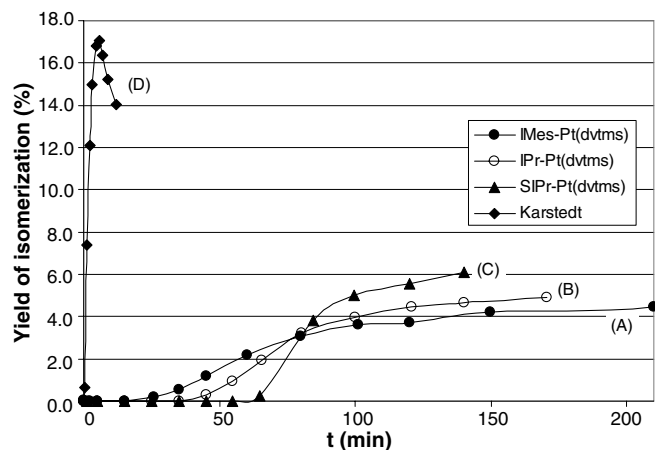
Fig. 2. Proposed catalytic cycle for the hydroosilylation of alkenes catalyzed by (NHC)Pt(dvtms) complexes.

These results can be nicely rationalized by the proposed mechanism depicted in Fig. 2. Indeed, the initiation step appears to proceed via a dissociative mechanism, in which a partial decooordination of the dvtms chelate occurs, followed by the subsequent hydroosilylation of the dvtms ligand to generate the highly reactive [NHC–Pt fragment] (II) (Scheme 3) [39].

The departure of this ligand, the slowest step of the whole process, requires the presence of the alkene (**13**) and the silane (**14**) to generate the transient intermediate – or transition state – (TS1). Insertion of the Si–H bond into the olefinic linkage leads to the platinum (II) derivative **12** which, after reductive elimination of **15**, affords the platinum (0) species **II**, probably stabilized by coordination to one or two alkenes [40]. Addition of the silane then regenerates the active complex or the transition state TS1 and a new catalytic cycle ensues. The steric bulk of the NHC li-



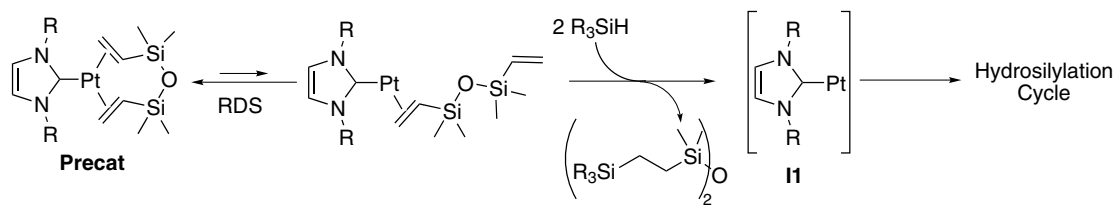
Graph 4. Isomerization (sum of all isomerized alkenes) of **14** catalyzed by (IMe)Pt(dvtms) curve (A), (ICy)Pt(dvtms) curve (B), (I'Bu)Pt(dvtms) curve (C) and Karstedt's catalyst curve (D).



Graph 5. Isomerization (sum of all isomerized alkenes) of **14** catalyzed by (IMes)Pt(dvtms) curve (A), (IPr)Pt(dvtms) curve (B) and (SIPr)Pt(dvtms) curve (C), and Karstedt's catalyst curve (D).

gand appears to play a key-role in two distinct stages of the reaction. In the initiation step, a high steric crowding will prevent the decooordination of one of the side arms of the dvtms ligand and its subsequent reaction with the silane. This results in a longer initiation step, as seen in Graph 3, which is especially apparent in the case of complexes **5**, **6** and **8**. Once the catalytically active [NHC–Pt] (II) fragment is freed from the dvtms ligand, the steric hindrance will benefit the catalytic activity by facilitating the reductive elimination of the Pt(silyl)(alkyl) intermediate **12** and by preventing catalyst deactivation [41].

It is important to note that the standard conditions chosen to evaluate and to compare the activity of the different catalysts are not the optimal ones. Under optimized conditions, the reaction always goes to completion (100% conversion of alkene) and gives less than 1% of the isomerization by-product.



Scheme 3. Proposed initiation process.

3. Conclusions

The analysis and structural characterization of an extended family of (NHC)Pt(0)(dvtms) complexes has allowed us to objectively compare the influence of a whole range of NHC ligands. The analysis of the principal bond distances, combined with other spectroscopic methods, indicated very little difference in bonding between all these ligands and the platinum center. It appears from these data, that the (NHC)–Pt(dvtms) complexes are “slow-release” precursors for an active platinum species. The rate of formation and the stability of the mono-ligated [NHC–Pt] fragment dictates the overall activity of the complex. This behavior can be partially rationalized in term of steric effect of the NHC ligand and ease of departure of the dvtms substituent.

Due to their ease of preparation (commercial availability of Karstedt’s catalyst), extended stability and high crystallinity, the NHC–Pt(dvtms) complexes serve as an ideal “platform” for the evaluation of the effects of carbene ligands on the platinum group metals. Another significant bonus brought by these complexes is the use of ^{195}Pt NMR to gain insight on the exact electronic nature of the metal center in these organometallic derivatives.

Work is currently in progress in our laboratory to understand in more detail the effect of the diene ligand on the reactivity of these species.

4. Experimental section

4.1. General information

^1H and ^{13}C NMR spectra were recorded either on a Varian Gemini 300 (200 and 50 MHz, respectively) or on a Gemini 2000 (300 and 75 MHz, respectively) as noted, and are internally referenced to residual protio solvent signals. The (107.54 MHz) spectra were measured with a Bruker Avance spectrometer equipped with a broad-band inverse probe with z -gradient. The ^{195}Pt spectra were recorded using g -HMBC sequence with a delay (d_6) for evolution of long range coupling of 125 ms ($d_6 = 1/J_{\text{Pt-H}}$). The ^{195}Pt spectra is externally referenced to H_2PtCl_6 in H_2O ($\delta = 0$ ppm). Data for ^1H are reported as follows: chemical shift (δ ppm), multiplicity (s = singlet, d = doublet, t = triplet, q = quartet, h = heptuplet, m = multiplet), integration, coupling constant (Hz) and assignment. Data

for ^{13}C NMR are reported in terms of chemical shift. IR spectra were recorded on a BIO-RAD FTS 135 spectrometer and are reported in terms of frequency of absorption (cm^{-1}). Mass spectra were obtained using Varian MAT-44 and Finnigan MATTSSQ 70 spectrometers with electron impact (70 eV) and chemical ionization (100 eV, ionization gas, isobutane). Gas liquid chromatography (GLC) was performed on a Thermo-Finnigan Trace GC chromatograph equipped with an FID detector using a Chrompack fused silica capillary column (CP Sil 8CB, 30 m \times 0.25 mm, DF = 0.25 μm).

1,3-Bis(2,6-diisopropylphenyl) imidazolium tetrafluoroborate (IPr-HBF₄) [42], 1,3-bis(2,4,6-trimethylphenyl) imidazolium tetrafluoroborate (IMes-HBF₄) [42], 1,3-bis(2,6-diisopropylphenyl)4,5-dihydroimidazolium tetrafluoroborate (SIPr-HBF₄) [43], 1,3-bis(*tert*-butyl) imidazolium tetrafluoroborate (I^tBu-HBF₄) [42], 1,3-bis(cyclohexyl) imidazolium tetrafluoroborate (ICy-HBF₄) [42], 1,3-dimethyl imidazolium iodide (IME-HI) [42], were prepared based on synthetic methods previously reported for each salt. The 1,3-dimethylbenzimidazolium iodide (BIMe-HI), 1,3-bis(methyl) benzimidazolium iodide (BImAllyl-HI) salt were obtained by classical double alkylation procedure of benzimidazole. The 1,3-bis(neopentyl) benzimidazolilydene (BINP) was synthesized following a procedure reported by Hahn et al. [24]. Karstedt’s catalyst [20] was synthesized according to the literature procedures. Divinyl tetramethyl disiloxane (dvtms) and bis(trimethylsiloxy)methylsilane (MD’M) were graciously donated by Rhodia Silicones.

4.2. General procedure for the synthesis of NHC–Pt(dvtms) complexes

To a suspension of the imidazolium salt (1 eq.) and Karstedt’s catalyst (16.2% of Pt in dvtms, 1 eq.), in toluene (0.5 M) under argon was added ^tBuOK(1.4 eq) at 0 °C. The reaction mixture was stirred at room temperature until the reaction was judged over by TLC (P.E./Et₂O 85:15), usually several hours. The mixture was then filtered on a pad of Celigel® (SiO₂/Celite 1:1) and eluted with P.E./Et₂O 85:15. Evaporation of the combined filtrates yielded the desired complex which crystallizes on standing. The complex could be further purified by flash chromatography (P.E./Et₂O 85:15). The crystals suitable for an X-ray diffraction study were grown from a saturated solution of ⁱPrOH.

4.2.1. *IMe–Pt(dvtms)* (1)

Yield: 77%. ^1H NMR (300 MHz, CDCl_3): $\delta = 7.00$ (s, 2H, $^4J_{\text{Pt-H}} = 11.8$ Hz, H_{Imi}), 3.54 (s, 6H, N-CH₃), 2.22 (d, 2H, $^3J = 10.3$ Hz, $^2J_{\text{Pt-H}^*} = 52.8$ Hz, C=CH_{2eq}), 2.02–1.71 (m, 4H, =CH_{2ax}=Si-CH=), 0.34 (s, 6H, Si-CH_{3seq}), -0.29 (s, 6H, SiCH_{3ax}); NMR ^{13}C (75 MHz, CDCl_3): $\delta = 179.8$ (Pt-C_{car}), 122.3 (C=C-N), 42.7 (C-Si), 40.7 (NCH₃), 34.5 (C=CHSi), 1.8 (SiCH_{3seq}), -1.4 (Si-CH_{3ax}); ^{195}Pt NMR (107 MHz, CDCl_3): $\delta = -5343$ ppm. IR (film, cm^{-1}): 2923 s, 1234 m, 1178 m, 992 m. MS (APCI): $m/z = 451-450-449$ [MH - vinyl]⁺, 293–292–291 [MH - dvtms]⁺, 97 [IMe - H]⁺.

4.2.2. *ICy–Pt(dvtms)* (2)

Yield: 90%. ^1H NMR (200 MHz, CDCl_3): $\delta = 7.24$ (s, 2H, $^4J_{\text{Pt-H}} = 12.6$ Hz, H_{Imi}), 4.30 (tt, 1H, $^3J_{\text{trans}} = 12.6$ Hz, $^3J_{\text{cis}} = 7.7$ Hz, N-CH), 4.19 (tt, 1H, $^3J_{\text{trans}} = 12.6$ Hz, $^3J_{\text{cis}} = 3.5$ Hz, N-CH), 2.17 (d, 2H, $^3J = 10.1$ Hz, $^2J_{\text{Pt-H}^*} = 53.1$ Hz, C=CH_{2eq}), 2.17–1.07 (m, 4H, Si-CH= + =CH_{2ax}), 0.31 (s, 6H, SiCH_{3seq}), -0.29 (s, 6H, Si-CH_{3ax}); NMR ^{13}C (50 MHz, CDCl_3): $\delta = 180.0$ ($^1J_{\text{Pt-C}} = 1350$ Hz, Pt-C_{car}), 118.0 (C=C-N), 59.4 ($^3J_{\text{Pt-C}} = 15$ Hz, NCH), 59.2 ($^3J_{\text{Pt-C}} = 15$ Hz, NCH), 41.2 ($^1J_{\text{Pt-C}} = 157.9$ Hz, C-Si), 34.6 (C_{cyclohexyl}), 34.5 ($^1J_{\text{Pt-C}} = 119.0$ Hz, C=CHSi), 25.4 (C_{cyclohexyl}), 25.3 s (C_{cyclohexyl}), 1.4 (Si-CH_{3seq}), -1.9 (SiCH_{3ax}); ^{195}Pt NMR (107 MHz, CDCl_3): $\delta = -5343$ ppm. IR (film, cm^{-1}): 3008 w, 2933 s, 1450 m, 1422 m, 1295 m, 1236 m, 1170 m, 992 s, 779 s. MS (APCI): $m/z = 587-586-585$ [MH - vinyl]⁺, 233 (100) [ICy - H]⁺. Anal. Calc. for C₂₃H₄₂N₂OPtSi₂: C, 45.00; H, 6.90; N, 4.56. Found: C, 44.95; H, 6.82; N, 4.47.

4.2.3. *tBu–Pt(dvtms)* (3)

Yield: 65%. ^1H NMR (200 MHz, CDCl_3): $\delta = 7.31$ (s, 1H, $^3J = 2.2$ Hz, $^4J_{\text{Pt-H}} = 12.0$ Hz, H_{Imi}), 7.30 (s, 1H, $^3J = 2.2$ Hz, $^4J_{\text{Pt-H}} = 12.0$ Hz, CH_{Imi}), 2.26 (d, 2H, $^3J = 11.0$ Hz, $^2J_{\text{Pt-H}^*} = 54$ Hz, C=CH_{2eq}), 1.88 (dd, 2H, $^3J = 11.4$ Hz, $^3J = 13.6$ Hz, Si-CH=), 1.74 (d, 2H, $^3J = 13.6$ Hz, $^2J_{\text{Pt-H}} = 52.2$ Hz, =CH_{2ax}), 1.60 (s, 9H, ^tBu), 0.31 (s, 6H, Si-CH_{3seq}), -0.28 (s, 6H, SiCH_{3ax}); NMR ^{13}C (50 MHz, CDCl_3): $\delta = 181.2$ ($^1J_{\text{Pt-C}} = 1360.8$ Hz, Pt-C_{car}), 118.2 ($^3J_{\text{Pt-C}} = 23.3$ Hz, C=C-N), 117.4 ($^3J_{\text{Pt-C}} = 23.3$ Hz, C=C-N), 58.8 ($^3J_{\text{Pt-C}} = 11.5$ Hz, C(CH₃)), 58.5 ($^3J_{\text{Pt-C}} = 11.5$ Hz, C(CH₃)₃), 46.7 ($^1J_{\text{Pt-C}} = 184.2$ Hz, C-Si), 32.0 ($^1J_{\text{Pt-C}} = 123.2$ Hz, C=CHSi), 31.0 (C(CH₃)₃), 30.6 (C(CH₃)₃), 1.6 (SiCH_{3seq}), -2.7 (SiCH_{3ax}); ^{195}Pt NMR (107 MHz, CDCl_3): $\delta = -5333$ ppm. IR (film, cm^{-1}): 1915 w, 1540 w, 1476 m, 1397 m, 1368 m, 1340 s, 1299 s, 1245 s, 1219 s, 1175 s, 1010 s, 977 s, 908 m, 845 s, 838 s, 778 s. MS (EI): $m/z = 562.1-561-560$ ([M]⁺), 318–317–316 (100) ([M - dvtms]⁺), 181 ([^tBu - H]⁺); m.p. = 189–191 °C.

4.2.4. *IAd–Pt(dvtms)* (4)

Yield: 66%. ^1H NMR (300 MHz, CDCl_3): $\delta = 7.30$ (d, 1H, $^3J = 2.3$ Hz, $^4J_{\text{Pt-H}^*} = 11.8$ Hz, H_{Imi}), 7.28 (s, 1H, $^3J = 2.3$ Hz, $^2J_{\text{Pt-H}^*} = 11.8$ Hz, CH_{Imi}), 2.35 (d, 2H, $^3J = 11.2$ Hz, $^2J_{\text{Pt-H}^*} = 53.2$ Hz, C=CH_{2eq}), 2.30–1.21 (m, 30H,

Si-CH= + =CH₂ + adamantyl), 0.34 (s, 6H, SiCH_{3seq}), -0.25 (s, 6H, SiCH_{3ax}); NMR ^{13}C (75 MHz, CDCl_3): $\delta = 180.3$ (Pt-C_{car}), 117.5 (C=C-N), 116.4 (C=C-N), 59.9 (N-C_{adamantyl}), 59.2 (N-C_{adamantyl}), 43.2 ($^1J_{\text{Pt-C}} = 185.4$ Hz, C-Si), 42.9 (CH_{adamantyl}), 42.5 (CH_{adamantyl}), 36.0 (CH_{adamantyl}), 31.4 ($^1J_{\text{Pt-C}} = 123.6$ Hz, C=CHSi), 30.2 (CH_{2adamantyl}), 30.0 (CH_{2adamantyl}), 1.8 (SiCH_{3seq}), -2.7 (SiCH_{3ax}); ^{195}Pt NMR (107 MHz, CDCl_3): $\delta = -5306$ ppm. IR (film, cm^{-1}): 2923 s, 1234 m, 1178 m, 992 m. MS (APCI): $m/z = 531-530-529$ [MH - dvtms]⁺, 337 [IAd - H]⁺.

4.2.5. *IMes–Pt(dvtms)* (5)

Yield: 85%. ^1H NMR (300 MHz, CDCl_3): $\delta = 7.12$ (s, 2H, $^4J_{\text{Pt-H}} = 9.2$ Hz, H_{Imi}), 6.86 (s, 4H, Mes), 2.25 (s, 6H, *p*-Me), 2.12 (s, 12H, *o*-Me), 1.93 (d, 2H, $^3J = 11.3$ Hz, $^2J_{\text{Pt-H}^*} = 55.0$ Hz, C=CH_{2eq}), 1.73–1.20 (m, 4H, Si-CH= + =CH₂ aq), 0.16 (s, 6H, SiCH_{3seq}), -0.77 (s, 6H, SiCH_{3ax}); NMR ^{13}C (75 MHz, CDCl_3): $\delta = 184.2$ (Pt-C_{car}), 138.6 (C_{arom.}), 136.9 (C_{arom.}), 135.4 (C_{arom.}), 129.1 (C_{arom.}), 128.9 (C_{arom.}), 123.0 ($^3J_{\text{Pt-C}} = 41.8$ Hz, C_{Im}), 41.3 ($^1J_{\text{Pt-C}} = 165.7$ Hz, C-Si), 35.3 ($^1J_{\text{Pt-C}} = 117.7$ Hz, C=CHSi), 21.1 (*p*-CH₃), 18.1 (*o*-CH₃), 1.6 (Si-CH_{3seq}), -2.5 (SiCH_{3ax}); ^{195}Pt NMR (107 MHz, CDCl_3): $\delta = -5339$ ppm. IR (film, cm^{-1}): 3134 m, 2964 s, 1488 m, 1322 m, 1246 m, 1179 m, 838 s, 784 s. MS (APCI): $m/z = 659-658-658$ [MH - CH=CH₂]⁺, 305 [IMes - H]⁺. Anal. Calc. for C₂₉H₄₂N₂OPtSi₂: C, 50.78; H, 6.17; N, 4.08. Found: C, 50.86; H, 6.14; N, 4.04.

4.2.6. *IPr–Pt(dvtms)* (6)

Yield: 70%. ^1H NMR (300 MHz, CDCl_3): $\delta = 7.35$ (t, 2H, $^3J = 7.7$ Hz, *p*-H_{Ph}), 7.20 (s, 2H, $^4J_{\text{Pt-H}} = 7.8$ Hz, H_{Imi}), 7.17 (d, 4H, $^3J = 7.7$ Hz, *m*-H_{Ph}), 2.97 (h, 4H, $^3J = 6.7$ Hz, CH(CH₃)₂), 1.51 (d, 2H, $^3J = 11.0$ Hz, $^2J_{\text{Pt-H}^*} = 54.1$ Hz, C=CH_{2eq}), 1.39–1.27 (m, 4H, Si-CH), 1.23 (d, 2H, $^3J = 13.2$ Hz, C=CH_{2ax}), 1.24 (d, 12H, $^3J = 6.7$ Hz, CH(CH₃)₂), 1.13 (d, 12H, $^3J = 6.7$ Hz, CH(CH₃)₂), 0.13 (s, 6H, SiCH_{3seq}), -0.76 (s, 6H, SiCH_{3ax}); NMR ^{13}C (75 MHz, CDCl_3): $\delta = 186.4$ (Pt-C_{car}), 146.0 (C_{arom.}), 136.9 ($^4J_{\text{Pt-C}} = 9.8$ Hz, C_{arom.}), 129.5 (C_{arom.}), 124.1 ($^3J_{\text{Pt-C}} = 42.0$ Hz, C_{Im}), 123.8 (C_{arom.}), 42.1 ($^1J_{\text{Pt-C}} = 166.5$ Hz, C-Si), 35.9 ($^1J_{\text{Pt-C}} = 120.9$ Hz, C=CHSi), 28.6 (CH(CH₃)₂), 26.0 (CH(CH₃)₂), 22.6 (CH(CH₃)₂), 1.8 (SiCH_{3seq}), -2.1 (SiCH_{3ax}); ^{195}Pt NMR (107 MHz, CDCl_3): -5340 ppm. IR (film, cm^{-1}): 3135 m, 2962 s, 1463 s, 1401 s, 1385 s, 1322 s, 1246 s, 1179 s, 1059 s, 977 s, 781 s. MS (APCI): $m/z = 744-743-742$ [MH - CH=CH₂]⁺, 579–578–577 [IPrNHC - Pt - 2H₂]⁺, 390 [IPr - H]⁺, 385 [IPr - H - 2H₂]⁺. Anal. Calc. for C₃₅H₅₄N₂OPtSi₂: C, 54.59; H, 7.07; N, 3.64. Found: C, 54.44; H, 7.10; N, 3.50.

4.3. General procedure for the synthesis of *SNHC–Pt(dvtms)* complexes

The 4,5-dihydroimidazol-2-ylidene platinum(0)(dvtms) complexes were synthesized and purified in an analogous

manner to the imidazol-2-ylidene platinum(0)(dvtms) complexes, apart that the corresponding carbene was generated in situ at 60 °C for 2 h instead of room temperature.

4.3.1. SIMes–Pt(dvtms) (7)

Yield: 50%. ¹H NMR (300 MHz, CDCl₃): δ = 6.83 (s, 4H, H_{Mes}), 4.00 (s, 4H, N–CH₂), 2.33 (s, 12H, *p*-Me), 2.22 (s, 6H, *o*-Me), 1.95 (d, 2H, ³J = 12.1 Hz, ²J_{Pt–H} = 55.0 Hz, =CH_{2eq}), 1.67 (d, 2H, ³J = 13.2 Hz, ²J_{Pt–H} = 55.5 Hz, =CH_{2ax}), 1.60–1.18 (m, 3H, Si–CH=), 0.87 (d, 1H, ³J = 13.2 Hz, ²J_{Pt–H} = 20.4 Hz, Si–CH=), 0.14 (s, 6H, SiCH_{3eq}), –0.80 (s, 6H, SiCH_{3ax}); NMR ¹³C (75 MHz, CDCl₃): δ = 211.0 (Pt–C_{car}), 137.6 (C_{arom.}), 136.9 (C_{arom.}), 135.9 (C_{arom.}), 129.1 (C_{arom.}), 51.2 (³J_{Pt–C} = 48.0 Hz, CH_{2Im}), 41.9 (¹J_{Pt–C} = 166.3 Hz, C–Si), 35.6 (¹J_{Pt–C} = 109.7 Hz, C=CHSi), 20.9 (*p*-CH₃), 18.0 (*o*-CH₃), 1.4 (SiCH_{3eq}), –2.8 (SiCH_{3ax}); ¹⁹⁵Pt NMR (107 MHz, CDCl₃): δ = –5365 ppm. IR (film, cm^{–1}): 3134 m, 2964 s, 1488 m, 1322 m, 1246 m, 1179 m, 838 s, 784 s. MS (APCI): *m/z* = 689–688–687 [MH]⁺, 673–672–671 [MH – CH₃]⁺, 660–659–658 [MH – CH=CH₂]⁺, 305 [SIMes – H]⁺.

4.3.2. SIPr–Pt(dvtms) (8)

Yield: 50%. ¹H NMR (300 MHz, CDCl₃): δ = 7.34 (t, 2H, ³J = 7.7 Hz, *p*-H_{Ph}), 7.2 (d, 4H, ³J = 7.7 Hz, *m*-H_{Ph}), 4.0 (s, 4H, H_{Imi}), 2.97 (h, 4H, ³J = 6.7 Hz, CH(CH₃)₂), 1.64 (d, 2H, ³J = 11.0 Hz, ²J_{Pt–H} = 50.6 Hz, =CH_{2eq}), 1.56–1.27 (m, 4H, Si–CH= + =CH_{2ax}), 1.24 (d, 12H, ³J = 6.7 Hz, CH(CH₃)₂), 1.22 (d, 12H, ³J = 6.7 Hz, CH(CH₃)₂), 0.07 (s, 6H, SiCH_{3eq}), –0.82 (s, 6H, SiCH_{3ax}); NMR ¹³C (75 MHz, CDCl₃): δ = 213.3 (Pt–C_{car}), 146.9 (C_{arom.}), 137.3 (C_{arom.}), 128.5 (C_{arom.}), 124.1 (C_{arom.}), 54.1 (³J_{Pt–C} = 48.4 Hz, CH_{2Im}), 43.0 (¹J_{Pt–C} = 169.2 Hz, C–Si), 36.8 (¹J_{Pt–C} = 112.8 Hz, C=CHSi), 28.6 (CH(CH₃)₂), 26.6 (CH(CH₃)₂), 23.3 (CH(CH₃)₂), 1.9 (SiCH_{3eq}), –2.3 (SiCH_{3ax}); ¹⁹⁵Pt NMR (107 MHz, CDCl₃): –5361 ppm. IR (film, cm^{–1}): 3067 w, 3030 w, 2962 s, 2929 s, 2869 s, 1588 w, 1472 s, 1445 s, 1413 s, 1386 m, 1364 m, 1322 s, 1303 s, 1278 s, 1245 s, 1180 s, 1106 w, 1055 m, 1010 s, 993 s, 910 s, 861 s, 838 s, 803 m, 782 s, 757 m, 733 s. MS (APCI): *m/z* = 745–744–743 [MH – CH=CH₂]⁺, 581–580–579 [IPr–Pt – 2H₂]⁺, 385 [IPr–H – 2H₂]⁺.

4.4. BIME–Pt(dvtms) (9)

Yield: 80%. ¹H NMR (200 MHz, CDCl₃): δ = 7.42–7.29 (m, 4H, Ph), 3.74 (s, 6H, ⁴J_{Pt–H} = 5.1 Hz, N–CH₃), 2.30 (dd, 2H, ³J = 10.9 Hz, ³J = 1.8 Hz, ²J_{Pt–H} = 54.1 Hz, C=CH_{2eq}), 2.22–1.81 (m, 4H, =CH_{2ax} + Si–CH=), 0.35 (s, 6H, SiCH_{3eq}), –0.23 (s, 6H, SiCH_{3ax}); NMR ¹³C (50 MHz, CDCl₃): δ = 199.5 (¹J_{Pt–C} = 1377.9 Hz, Pt–C_{car}), 135.7 (³J_{Pt–C} = 39.0 Hz, C=C–N), 122.1 (C_{arom.}), 108.9 (⁴J_{Pt–C} = 9.6 Hz, C_{arom.}), 40.7 (¹J_{Pt–C} = 155.7 Hz, C–Si), 35.6 (¹J_{Pt–C} = 113.7 Hz, C=CHSi), 33.4 (³J_{Pt–C} = 47.2 Hz, NCH₃), 33.3 (³J_{Pt–C} = 47.1 Hz, NCH₃), 1.5 (SiCH_{3eq}), –1.9 (SiCH_{3ax}); ¹⁹⁵Pt NMR (107 MHz, CDCl₃):

δ = –5379 ppm. IR (film, cm^{–1}): 3009 w, 1391 m, 1241 m, 1174 w, 830 s, 776 s. MS (E.I.) *m/z* = 528–527–526 ([M]⁺); 513–512–511 ([M – CH₃]⁺), 501–500–499 ([M – HC=CH₂]⁺), 341–340–339 ([M – dvtms]⁺), 147 ([BIME – H]⁺).

4.4.1. BI_nPr–Pt(dvtms) (10)

Yield = 83%. ¹H NMR (200 MHz, CDCl₃): δ = 7.36–7.20 (m, 4H, Ph), 4.15–4.07 (m, 4H, CH₂N), 2.28 (dd, 2H, ³J = 10.2 Hz, ³J = 1.7 Hz, ²J_{Pt–H} = 54.1 Hz, C=CH_{2eq}), 2.07–1.65 (m, 8H, Si–CH= + =CH₂ + CH₂Me), 0.90 (t, 3H, ³J = 7.4 Hz, ₃), 0.87 (t, 3H, ³J = 7.4 Hz, CH₃), 0.33 (s, 6H, SiCH_{3eq}), –0.25 (s, 6H, SiCH_{3ax}); ¹³C NMR (50 MHz, CDCl₃): δ = 198.3 (¹J_{Pt–C} = 1373.3 Hz, Pt–C_{car}), 135.1 (³J_{Pt–C} = 41.6 Hz, C=CN), 121.8 (C_{arom.}), 109.4 (⁴J_{Pt–C} = 8.3 Hz, C_{arom.}), 49.0 (³J_{Pt–C} = 40.0 Hz, NCH₃), 48.9 (³J_{Pt–C} = 40.4 Hz, NCH₃), 43.3 (¹J_{Pt–C} = 158.2 Hz, C–Si), 35.1 (¹J_{Pt–C} = 113.6 Hz, C=C–Si), 22.6 (CH₂Me), 22.4 (CH₂Me), 11.3 (CH₃), 11.2 (CH₃), 1.4 (SiCH_{3eq}), –1.9 (SiCH_{3ax}); ¹⁹⁵Pt NMR (107 MHz, CDCl₃): δ = –5383 ppm. IR (KBr, cm^{–1}): 1610, 1579, 1428, 1402, 1298, 1245, 1175, 990, 860, 836, 785, 741, 573. MS (E.I.) *m/z* = 584–583–582 (M⁺), 569–568–567 ([M – CH₃]⁺), 556–555–554 ([M – HC=CH₂]⁺), 394–393 –392 ([M – dvtms – 2H₂]⁺), 203 ([BI_nPr – H]⁺); m.p. = 184–186 °C. Anal. Calc. for C₂₁H₃₆N₂OPtSi₂: C, 43.21; H, 6.22; N, 4.80. Found: C, 43.12; H, 6.16; N, 4.81.

4.4.2. BI_mAllyl–Pt(dvtms) (11)

Yield = 78%. ¹H NMR (200 MHz, CDCl₃): δ = 7.33–7.22 (m, 4H, Ph), 4.95 (s, 2H, C=CH₂), 4.85 (s, 4H, CH₂N), 4.73 (s, 1H, C=CH₂), 4.55 (s, 1H, C=CH₂), 2.32 (dd, 2H, ³J = 10.6 Hz, ³J = 1.3 Hz, ²J_{Pt–H} = 54.3 Hz, C=CH_{2eq}), 2.1–1.1.8 (m, 4H, Si–CH + =CH_{2ax}), 1.70 (s, 3H, CH₃), 1.68 (s, 3H, CH₃), 0.35 (s, 6H, SiCH_{3eq}), –0.26 (s, 6H, SiCH_{3ax}); ¹³C NMR (50 MHz, CDCl₃): δ = 198.3 (¹J_{Pt–C} = 1398.3 Hz, Pt–C_{car}), 139.8 (MeC=), 139.3 (MeC=), 135.3 (³J_{Pt–C} = 41.6 Hz, C=C–N), 122.1 (C_{arom.}), 112.7 (=CH₂), 111.8 (=CH₂), 110.1 (C_{arom.}), 53.1 (³J_{Pt–C} = 42.6 Hz, NCH₂), 52.9 (³J_{Pt–C} = 42.8 Hz, NCH₂), 42.1 (¹J_{Pt–C} = 155.4 Hz, C–Si), 35.9 (¹J_{Pt–C} = 113.6 Hz, C=CHSi), 20.0 (CH₃), 1.4 (SiCH_{3eq}), –1.9 (SiCH_{3ax}); IR (KBr, cm^{–1}): 1663, 1480, 1427, 1401, 1299, 1240, 1225, 1174, 981, 905, 884, 838, 780, 739. MS (E.I.) *m/z* = 607–606–605 ([M]⁺); 421–420–419 ([M – dvtms]⁺).

4.4.3. BI_nP–Pt(dvtms) (12)

The corresponding thiourea (1 eq.) was reduced over Na/K amalgam in degassed *o*-xylene for 20 days at room temperature. The reaction mixture was filtered over celite under Ar. To this mixture was added a commercial solution of Karstedt's catalyst (1 eq., 16.7% of Pt in xylenes). The reaction mixture was stirred overnight. It was then diluted with DCM, washed with water and filtered on deactivated alumina using DCM as the eluent. Evaporation yielded white crystals. Yield = 50%. ¹H NMR (200 MHz,

CDCl₃): δ = 7.51–7.43 (m, 2H, Ph), 7.30–7.21 (m, 2H, Ph), 4.25 (s, 2H, $^4J_{\text{Pt-H}} = 5.8$ Hz, N-CH₂), 4.17 (s, 2H, $^4J_{\text{Pt-H}} = 5.8$ Hz, N-CH₂), 2.42 (t, 2H, $^3J = 6.0$ Hz, $^2J_{\text{Pt-H}} = 55.0$ Hz, C=CH_{2eq}), 2.41 (d, 4H, $^3J = 6.0$ Hz, $^2J_{\text{Pt-H}} = 51.0$ Hz, Si-CH=CH_{2ax}), 1.02 (s, 9H, C(CH₃)₃), 0.95 (s, 9H, C(CH₃)₃), 0.39 (s, 6H, SiCH_{3eq}), -0.16 (s, 6H, SiCH_{3ax}); ¹³C NMR (50 MHz, CDCl₃): δ = 201.9 ($^1J_{\text{Pt-C}} = 1337.0$ Hz, Pt-C_{car}), 135.9 ($^3J_{\text{Pt-C}} = 40.7$ Hz, C=C-N), 121.3 (C_{arom.}), 111.2 ($^4J_{\text{Pt-C}} = 9.0$ Hz, C_{arom.}), 111.1 ($^4J_{\text{Pt-C}} = 9.0$ Hz, C_{arom.}), 58.7 ($^3J_{\text{Pt-C}} = 55.4$ Hz, NCH₂), 58.5 ($^3J_{\text{Pt-C}} = 57.2$ Hz, NCH₂), 43.8 ($^1J_{\text{Pt-C}} = 173.3$ Hz, C-Si), 35.1 ($^1J_{\text{Pt-C}} = 114.0$ Hz, C=CHSi), 34.0 (C(CH₃)₃), 33.8 (C(CH₃)₃), 29.5 (C(CH₃)₃), 29.3 (C(CH₃)₃), 1.6 (SiCH_{3eq}), -1.9 (SiCH_{3ax}); IR (KBr, cm⁻¹): 1611, 1478, 1398, 1376, 1339, 1239, 1177, 1159, 1009, 996, 862, 836, 778, 737. MS (E.I.) m/z = 640–639–638 ([M]⁺), 625–624–623 ([M - CH₃]⁺); 259 ([BInP]⁺); m.p. = 142–144 °C.

4.5. General procedure for the hydrosilylation reaction

A 0.5% weight per volume stock solution of each N-heterocyclic carbene platinum(0) complexes in toluene is prepared and used for the precise addition of the catalyst. A three-necked 100 ml round-bottomed flask was loaded with 1-octene (5 g, 45 mmol), MD'M (9 g, 45 mmol), dodecane (5 g, GC internal standard) and 56 g of *o*-xylene (63 ml). The reaction vessel was heated at 72 °C and was thermally equilibrated for 1–2 h. The catalyst was injected

(0.005 mol%) and the progress of the reaction was monitored from that instant. Samples (2–3 drops) were taken regularly (every 5–15 min) and eluted with dichloromethane (2 ml) on a small column of activated charcoal, before being analyzed by GC. The response coefficients were measured for reactants and products against dodecane.

4.6. X-ray structure analysis of 5, 8, 9 and 11

The X-ray intensity data were measured at room temperature for all the four compounds. The data were collected with a MAR345 image plate using Mo K α ($\lambda = 0.71069$ Å) radiation. The crystal data and the data collection parameters are summarized in Table 8. The unit cell parameters were refined using all the collected spots after the integration process. The data were not corrected for absorption but the data collection mode (87, 200, 156 and 100 images, respectively, of 5, 8, 9 and 11, $\Delta\Phi = 3^\circ$, giving a large number of measurements for each reflection) partially takes the absorption phenomena into account.

The four structures were solved by Patterson or direct methods with SHELXS97(1), and refined by full-matrix least-squares on F^2 using SHELXL97 [44]. All the non-hydrogen atoms were refined anisotropically. The hydrogen atoms were calculated with AFIX and included in the refinement with a common isotropic temperature factor. The details of the refinement and the final R indices are presented in Table 8. In each structure, the largest peak in the final Fourier difference synthesis is located near a Pt atom.

Table 8
Crystallographic data for 5, 8, 9 and 11

	5	8	9	11
Formula	C ₂₉ H ₄₂ N ₂ O ₂ PtSi ₂	C ₃₅ H ₅₆ N ₂ O ₂ PtSi ₂	C ₁₇ H ₂₈ N ₂ O ₂ PtSi ₂	C ₂₃ H ₃₆ N ₂ O ₂ PtSi ₂
M_r	685.92	772.09	527.68	607.80
System	Monoclinic	Triclinic	Monoclinic	Triclinic
Space group	$P2_1/n$	$P\bar{1}$	$P2_1/c$	$P\bar{1}$
a (Å)	13.013(4)	10.411(5)	8.060(3)	10.202(3)
b (Å)	18.214(5)	19.355(7)	20.038(8)	11.289(4)
c (Å)	13.466(4)	21.520(8)	12.837(5)	11.933(4)
α (°)	90	63.93(2)	90	84.51(2)
β (°)	104.84(2)	82.74(2)	100.79(2)	82.35(2)
γ (°)	90	77.79(2)	90	71.81(2)
V (Å ³)	3085(2)	3804(2)	2037(1)	1291.9(7)
D_x (g cm ⁻³)	1.48	1.35	1.72	1.56
Z	4	4	4	2
Crystal size (mm)	0.20 × 0.20 × 0.10	0.20 × 0.20 × 0.15	0.32 × 0.24 × 0.20	0.30 × 0.25 × 0.20
μ (mm ⁻¹)	4.65	3.78	7.01	5.54
Number of reflections collected	70475	31868	29436	28497
R_{int}	0.058	0.047	0.051	0.066
θ Range (°)	3.0–50.7	2.5–48.8	2.6–55.0	2.4–55.0
Number of unique reflections	5606	11974	4505	5831
Number of observed reflections [$I > 2\sigma(I)$]	5307	10674	4408	5454
Completeness (%)	98.9	95.5	96.1	97.7
Number of parameters	318	741	216	282
Goodness of fit or F^2	1.13	1.07	1.27	1.09
R for observed reflections	0.031	0.034	0.041	0.039
ωR_2	0.089	0.086	0.103	0.104
Largest differential peak and hole (e Å ⁻³)	1.29/–1.30	0.65/–0.68	2.27/–2.58	1.40/–1.72

Crystallographic data for the structures reported in this paper and previously published structures have the following Cambridge Crystallographic Data Centre as supplementary publication CCDC-197066 (**1**) [18], CCDC-261192 (**3**), CCDC-261192 (**2**) [19], CCDC-275306 (**5**), CCDC-275307 (**8**), CCDC-275308 (**9**), CCDC-275309 (**11**) and CCDC-271531 (**12**). Copies of the data can be obtained free of charge on application to CCDC, 12 Union Road, Cambridge CB2 1EZ, UK (fax: (+44)1223 336 033; e-mail: deposit@ccdc.cam.ac.uk).

Acknowledgements

Financial support by the Université catholique de Louvain, Rhodia Silicones and Rhodia Corporate is gratefully acknowledged. I.E.M. is thankful to Rhodia for receiving the 2002 Rhodia Outstanding Award.

References

- [1] H.-W. Wanzlick, *Angew. Chem.* 74 (1962) 129.
- [2] H.-W. Wanzlick, *Angew. Chem. Int. Ed.* 1 (1962) 75.
- [3] H.-W. Wanzlick, H.J. Schönherr, *Angew. Chem. Int. Ed.* 7 (1968) 141.
- [4] H.-W. Wanzlick, H.J. Schönherr, *Angew. Chem.* 80 (1968) 154.
- [5] K. Öfele, *J. Organomet. Chem.* 12 (1968) P42–P43.
- [6] P.J. Cardin, B. Cetinbaya, M.F. Lappert, *Chem. Rev.* 72 (1972) 545.
- [7] M.F. Lappert, R.K. Maskell, *J. Organomet. Chem.* 264 (1984) 217.
- [8] A. Igau, H. Grützmacher, A. Baceiredo, G. Bertrand, *J. Am. Chem. Soc.* 110 (1988) 6463–6466.
- [9] A.J.J.I. Arduengo, R.L. Harlow, M. Kilne, *J. Am. Chem. Soc.* 113 (1991) 361.
- [10] W.A. Herrmann, *Angew. Chem. Int. Ed.* 41 (2002) 1290.
- [11] A.C. Hillier, G.A. Grasa, M.S. Viciu, H.M. Lee, C. Yang, S.P. Nolan, *J. Organomet. Chem.* (2002) 653.
- [12] N.M. Scott, S.P. Nolan, *Eur. J. Inorg. Chem.* (2005) 1815.
- [13] D.R. Jensen, M.J. Schultz, J.A. Mueller, M.S. Sigman, *Angew. Chem. Int. Ed.* 42 (2003) 3810.
- [14] T. Hiyama, T. Kusumoto, in: B.M. Trost, I. Fleming (Eds.), *Comprehensive Organic Synthesis*, vol. 8, Pergamon Press, Oxford, 1991, p. 763.
- [15] J.L. Speier, *Adv. Organomet. Chem.* 17 (1979) 407.
- [16] B. Marciniec, J. Gulinski, W. Urbaniac, Z.W. Kornetka, *Comprehensive Handbook on Hydrosilylation*, Pergamon, Oxford, UK, 1992.
- [17] J. Stein, L.N. Lewis, Y. Gao, R.A. Scott, *J. Am. Chem. Soc.* 121 (1999) 3693.
- [18] I.E. Markó, S. Stérin, O. Buisine, G. Mignani, P. Branlard, B. Tinant, J.-P. Declercq, *Science* 298 (2002) 204.
- [19] I.E. Markó, G. Michaud, G. Berthon-Gelloz, O. Buisine, S. Stérin, *Adv. Synth. Catal.* (2004) 1429.
- [20] B.D. Karstedt, *General Electric*, US Pat. 3,715,334, 1973.
- [21] W.A. Herrmann, C. Köcher, J.L. Goossen, G.R.J. Artus, *Chem. Eur. J.* 2 (1996) 1627.
- [22] G. Chandra, P.Y. Lo, P.B. Hitchcock, M.F. Lappert, *Organometallics* 6 (1986) 191.
- [23] A.R. Chianese, X. Li, M.C. Janzen, J.W. Faller, R.H. Crabtree, *Organometallics* 22 (2003) 1663.
- [24] F.E. Hahn, L. Wittenbecher, R. Boese, D. Bläser, *Chem. Eur. J.* 5 (1999) 1931.
- [25] P.S. Pregosin, *Coord. Chem. Rev.* 44 (1982) 247.
- [26] P.B. Hitchcock, M.F. Lappert, N.J.W. Warhurst, *Angew. Chem. Int. Ed.* 30 (1991) 438.
- [27] N.J.W. Warhurst, University of Sussex, Sussex, UK, 1990.
- [28] O. Buisine, G. Berthon-Gelloz, J.-F. Brière, S. Stérin, G. Mignani, P. Branlard, B. Tinant, J.-P. Declercq, I.E. Markó, *Chem. Commun.* (2005) 3856.
- [29] F.R. Hartley, in: E.W. Abel, F.G.A. Stone, G. Wilkinson (Eds.), *Comprehensive Organometallic Chemistry*, vol. 6, Pergamon, Oxford, UK, 1982, p. 614.
- [30] M.S. Viciu, O. Navarro, R.F. Germaneau, R.A. Kelly III, W. Sommer, N. Marion, E.D. Stevens, L. Cavallo, S.P. Nolan, *Organometallics* 23 (2004) 1629.
- [31] W.A. Herrmann, M. Elison, J. Fisher, C. Köcher, G.R.J. Artus, *Angew. Chem. Int. Ed.* 34 (1995) 2371.
- [32] D.S. McGuinness, K.J. Cavell, *Organometallics* 18 (1999) 1596.
- [33] We have observed an increase in selectivity for the hydrosilylation of alkynes with aryl substituted NHCs.
- [34] Vinyl silanes are excellent ligands for late low-valent transition metals. It has been suggested that the coordinating ability of vinyl silanes is mostly due to the Si=C ($d\pi-p\pi$) interaction, which allows delocalization of the alkene's electron density onto the silicon atom via its d-orbitals. This results in enhanced back-bonding between the metal center and the olefin delocalized π^* orbital. Therefore, greater thermal stability of the vinylsilane-containing complex relative to their carbon analogue is observed.
- [35] P. Steffanut, J.A. Osborn, A. DeCian, J. Fisher, *Chem. Eur. J.* 4 (1998) 2008.
- [36] G. Beuter, O. Heyke, I.P. Lorenz, *Z. Naturforsch., B: Chem. Sci.* 46 (1991) 1694.
- [37] R. Dorta, E.D. Stevens, N.M. Scott, C. Costabile, L. Cavallo, C.D. Hoff, S.P. Nolan, *J. Am. Chem. Soc.* 127 (2005) 2485.
- [38] Further details on the involvement of such common intermediate will be given in a forthcoming paper.
- [39] Interestingly the length of the C=C of the dtvms ligand in these Pt(0) complexes can be directly correlated to the activity of these catalysts in the hydrosilylation reaction. The shorter the C=C bond, the higher the activity of the catalyst. This observation further reinforces our suggestion suggests that the decoordination of the dtvms ligand is the rate determining step in the generation of the active catalyst.
- [40] The reaction displays saturation kinetics. Whilst increasing the concentration of the alkene leads initially to an enhanced reaction rate, the presence of a large excess of olefin eventually results in a partial inhibition of the hydrosilylation reaction, probably arising from the saturation of the coordination sphere of the platinum complex **II**.
- [41] The rate of the hydrosilylation reaction appears to be first order in the alkene **14** and in the silane **13**, implying that both partners are involved at the same time in the "rate determining step" of the catalytic cycle. Interestingly, incubation of Cy-NHC-Pt(dtvms) complex with excess alkene does not promote the exchange between the dtvms ligand and the olefin. In contrast, treatment of the same complex with excess silane generates the corresponding N-heterocyclic platinum (II) silyl hydride dimer. This dimer is, however, a less efficient catalyst than the parent complex. For the preparation and structure determination of the analogous phosphine-containing dimers, see: M. Ciriano, M. Green, J.A.K. Howard, J. Proud, J.L. Spencer, G.A.F. Stone, C.A. Tsipis, *J. Chem. Soc., Dalton Trans.* (1978) 801; For the hydrosilylation of alkenes using these dimers, see: M. Green, J.L. Spencer, G.A.F. Stone, C.A. Tsipis, *J. Chem. Soc., Dalton Trans.* (1977) 1519.
- [42] J. Huang, S.P. Nolan, *J. Am. Chem. Soc.* 121 (1999) 9889.
- [43] A.J.J.I. Arduengo, R. Krafczyk, R. Schmutzler, H.A. Craig, J.R. Goerlich, W.J. Marshall, M. Unverzagt, *Tetrahedron* 55 (1999) 14523.
- [44] G.M. Sheldrick, *SHELXL-1997: Program for Crystal Structure Determination and Refinement*, University of Göttingen, Göttingen, Germany, 1997.